

The Genetic Risk in Mice from Radiation: An Estimate of the Mutation Induction Rate per Genome

Authors: Asakawa, Jun-ichi, Kodaira, Mieko, Cullings, Harry M., Katayama, Hiroaki, and Nakamura, Nori

Source: Radiation Research, 179(3) : 293-303

Published By: Radiation Research Society

URL: <https://doi.org/10.1667/RR3095.1>

BioOne Complete (complete.BioOne.org) is a full-text database of 200 subscribed and open-access titles in the biological, ecological, and environmental sciences published by nonprofit societies, associations, museums, institutions, and presses.

Your use of this PDF, the BioOne Complete website, and all posted and associated content indicates your acceptance of BioOne's Terms of Use, available at www.bioone.org/terms-of-use.

Usage of BioOne Complete content is strictly limited to personal, educational, and non - commercial use. Commercial inquiries or rights and permissions requests should be directed to the individual publisher as copyright holder.

BioOne sees sustainable scholarly publishing as an inherently collaborative enterprise connecting authors, nonprofit publishers, academic institutions, research libraries, and research funders in the common goal of maximizing access to critical research.

The Genetic Risk in Mice from Radiation: An Estimate of the Mutation Induction Rate per Genome

Jun-ichi Asakawa,^{a,1} Mieko Kodaira,^a Harry M. Cullings,^b Hiroaki Katayama^c and Nori Nakamura^a

Departments of ^aGenetics, ^b Statistics, and ^c Information Technology, Radiation Effects Research Foundation, 5-2 Hijiyama Park, Minami-ku, Hiroshima 732-0815, Japan

Asakawa, J., Kodaira, M. N., Katayama, H., Cullings, H. and Nakamura N. The Genetic Risk in Mice from Radiation: An Estimate of the Mutation Induction Rate per Genome *Radiat. Res.* 179, 293–303 (2013).

Restriction Landmark Genome Scanning (RLGS) is a method that uses end-labeled ³²P *NotI* sites that are mostly associated with coding genes to visualizes thousands of DNA fragments as spots in two-dimensional autoradiograms. This approach allows direct detection of autosomal deletions as spots with half normal intensity. The method was applied to mouse offspring derived from spermatogonia exposed to 4 Gy of X rays. A genome-wide assessment of the mutation induction rate was estimated from the detected deletions. Examinations were made of 1,007 progeny (502 derived from control males and 505 from irradiated males) and 1,190 paternal and 1,240 maternal spots for each mouse. The results showed one deletion mutation in the unirradiated paternal genomes of 502 offspring (0.2%) and 5 deletions in the irradiated paternal genomes of 505 offspring (1%). The difference was marginally significant, with the deletion sizes ranged from 2–13 Mb. If the frequencies are taken at face value, the net increase was 0.8% after an exposure of 4 Gy, or 0.2% per Gy per individual if a linear dose response is assumed. Since the present RLGS analysis examined 1,190 *NotI* sites, while the mouse genome contains ~25,000 genes, the genomic probability of any gene undergoing a deletion mutation would be 25× 0.2%, or 5% per Gy. Furthermore, since the present RLGS screened about 0.2% of the total genome, the probability of detecting a deletion anywhere in the total genome would be estimated to be 500 times 0.2% or 100% (i.e., 1 deletion per Gy). These results are discussed with reference to copy number variation in the human genome. © 2013 by Radiation Research Society

INTRODUCTION

Exposure to ionizing radiation increases the risk of developing various diseases, including cancer and non-cancer diseases (1–3). When germ cells are exposed to radiation, the risk of hereditary disorders may be increased. As the genetic effects of radiation have been confirmed in various species, it is unlikely that humans are an exception. Nevertheless, no clear evidence has been obtained for radiation-induced germline mutations among the offspring of atomic-bomb (A-bomb) survivors (4), or of those of childhood cancer survivors (5, 6).

Among the past studies on the genetic effects of radiation in animals, specific-locus tests in mice are the most comprehensive. The experiments were primarily conducted by Russell's group (7 loci) at the Oak Ridge National Laboratory and to a lesser extent by Lyon's group (6 loci) at the Medical Research Council in Harwell. Through the studies, it was recognized that the mean mutation induction rate found by Russell's group at the 7 loci was 2.76×10^{-5} /locus per Gy (*a*, *se*, *c*, *b*, *p*, *d* and *s*) and was considerably higher than the rate obtained by the Lyon's group of 0.86×10^{-5} /locus per Gy at the *a*, *bp*, *pa*, *fz*, *ln* and *pe* loci (7). Such a difference in radiation sensitivity among loci makes it hard to estimate the mean mutation induction rate in the genome. Summarizing the data, the current UNSCEAR Report suggests the mean mutation induction rate at 36 genes is 1.08×10^{-5} /locus per Gy, which was nearly one-half of the mean in the 7 loci study (7).

To better understand the mean mutation induction rate per genome, it would be necessary to examine a large number of genes per individual concurrently. For this purpose, previous studies have used the restriction landmark genome scanning (RLGS) method for analysis of mouse offspring born to X-irradiated parents (8). This method can visualize and screen about 2,000 DNA fragments (end-labeled with ³²P after digestion of genomic DNA with specific restriction enzymes) as spots on a two-dimensional autoradiogram. This technique results in reproducible intensities and low coefficients of variation (CV) of ≤ 0.12 (9), that allow a deletion mutation for a heterozygous fragment to be detected as a decreased spot intensity of about 50%. The

Editor's note. The online version of this article (DOI: 10.1667/RR3095.1) contains supplementary information that is available to all authorized users.

¹Address for correspondence: Department of Genetics, Radiation Effects Research Foundation, 5-2 Hijiyama Park, Minami-ku, Hiroshima, 732-0815, Japan; e-mail: jun@rerf.or.jp.

rate of false negatives (the probability of missing mutations) is estimated as about 3% (9), and the rate of false positives (the probability of detecting normal sequences as mutations) is kept very low, because nearly all of the mutation candidates can be confirmed by additional means. The method does not require probes for mutation detection, while the nature of mutations can usually be studied by cloning and sequencing the wild-type allele or mutant allele.

In our previous study, the BALB/c strain of mice was used for both parents, and *NotI* enzyme (GC/GGCCGC) was used to end-label DNA to mark GC-rich sequences in the genome (8). We considered it desirable to screen DNA fragments that are primarily related to functional genes rather than fragments with unknown functions. We postulated that because mutations in functional genes would be more likely to result in phenotypic changes, and hence would be more significant as a hereditary risk after radiation exposure. The *NotI* sites are disproportionally located at unmethylated "CpG islands", that are common upstream of genes and are thought to be associated with functional genes. Thus, we and others propose that the use of *NotI* as the landmark enzyme in the RLGS will result in the delivery of a high proportion of visualized spots from active genes (10, 11). Our study gave rise to only 4 deletion mutations and the results indicated that the maximum induction rate of deletion mutations was 0.2×10^{-5} /locus per Gy (8). This result was close to the proposed rate of 0.3×10^{-5} /locus per Gy (7) with 30% of the specific-locus mutation comprised large deletions.

To obtain more information on the mutation induction rate at different parts of the genome, a second study was conducted to measure the mutation rate at AT-rich sequences in the genome (12). In this study, *AflIII* (recognition sequence: C/TTAAG) was used as the landmark enzyme for radiolabeling of the DNA fragments. This method was found to specifically visualize AT-rich DNA fragments as spots. Unfortunately, normal alleles of most of the mutated spots contained repeat sequences (e.g., satellite, SINE, LINE and short tandem repeat sequences) and therefore presented as multiple copies in the genome, which prevented us from characterizing the mutations. None the less, the estimated mutation rate was 0.6×10^{-5} /locus per Gy, which is in the same range as that estimated at GC-rich sequences. In addition, we found 3 possible deletions free from the repeat sequences among 184 offspring (514 spots per individual) derived from 5 Gy irradiated spermatogonia with no corresponding mutations in the control group. Unfortunately, since the same strain of mice (BALB/c) was used for both parents in the first study, parental origins of the mutations could not be determined. Further, that study raised a possibility that the results obtained might not represent conditions in wild-type animals because the BALB/c strain bears a mutation in a gene involved in DNA repair (DNA-PKcs) (13). To overcome these caveats in the present study, we used male hybrids of C57BL/6 and C3H/He strains (abbreviated as

B6C3) for irradiation, and females from the JF1 strain (a strain somewhat remote from laboratory mice). Mated the JF1 females with the irradiated B6C3 males allowed the parental origin of mutations to be determined.

MATERIALS AND METHODS

Mice

B6C3 male mice (8 weeks old) were purchased from Charles River Japan. The JF1 strain was derived from a Japanese Fancy Mouse that originated from a Japanese wild mouse (*Mus musculus molossinus*), and which was established at the National Institute of Genetics (NIG, Mishima, Japan) (14). The animals were kindly supplied by Dr. T. Shiroishi at the NIG. Thirteen 10-week-old male mice were exposed to 4 Gy of X rays. During irradiation, each male mouse was immobilized on a styrofoam plate (ventral side up), and the body, except for the testes, was shielded with a 3-mm-thick lead plate. The X rays were given vertically by a Shimadzu X-ray generator, operated at 220 kVp and 8.0 mA through a 0.5 mm aluminum and 0.3 mm copper filter at a dose rate of 1.19 Gy/min. After an 8-week recovery period, the mice were individually mated with 3 JF1 females to collect offspring derived from irradiated spermatogonia cells. The offspring from these crosses constituted the exposed group. The F₁ mice born to the unirradiated B6C3 males (22 animals) and the JF1 females (66 animals) constituted the control group. When the offspring reached approximately 6 weeks of age, they were sacrificed, and their spleens, livers and kidneys were removed and stored at -80°C until use. A part of the spleen was used before cryopreservation to extract high-molecular-weight DNA for the screening. When putative mutations were detected, kidney and liver DNA samples were used to confirm the experimental findings. Experiments were carried out according to the standard protocols employed at the Radiation Effects Research Foundation (RERF). Mice were housed and cared for at the RERF animal care facility and the study plan was approved by the in-house Animal Care Committee.

Restriction Landmark Genome Scanning (RLGS)

DNA was prepared, labeled and electrophoresed as described (9, 15, 16). Briefly, genomic DNA was double digested with *NotI* (GC/GGCCGC) and *EcoRV* (GAT/ATC) restriction enzymes. The 4-base 5' overhangs produced by the *NotI* digestion were end-labeled with ^{32}P -dCTP and ^{32}P -dGTP with a fill-in reaction with a polymerase so that only DNA fragments containing the cleaved *NotI* ends were quantitatively visualized. The DNA digests were then separated by a two-step electrophoresis. For the first-dimension electrophoresis, two types of 61-cm-long agarose gel casts were prepared, 0.9% and 0.8% gel, for an optimal separation of 1–5 kb and 5–10 kb *NotI*-*EcoRV* fragments, respectively. Subsequently, the *NotI*-*EcoRV*-digested DNA fragments were further digested *in situ* with a third restriction enzyme, *HinfI* (G/ANTC), and the agarose gels were placed on top of the second-dimensional polyacrylamide gels for separation of the fragments. The gels were then dried and subjected to autoradiography.

Measurements of Spot Intensities

Details of spot intensity measurements have been described previously (9, 17). Briefly, autoradiograms were scanned and digitized images were obtained using a laser film scanner (Abe-Sekkei, Tokyo, Japan). For each selected spot in a study sample, a mean intensity of 10 neighboring spots was used to calculate the ratio of spot intensities between the study gel and the master gel to compensate locally for any variation in the degree of background darkness of each autoradiogram. For this calculation, the two largest and two smallest values were ignored, and the remaining 6 ratios were averaged. The raw value of

the spot intensity was divided by this local average to obtain the adjusted spot intensity (9, 17).

Molecular Analysis

Cloning and sequencing. To recover normal DNA fragments from the spots which had undergone mutations, genomic DNA from a mouse that showed no mutations was first digested with *NotI* and *EcoRV*. The digested DNA (the *NotI* sites were not filled in) were subjected to selection procedures for enrichment of fragments that contained *NotI* sites (9). The enriched nonlabeled DNA fragments were then mixed with ordinarily radiolabeled fragments, and the mixed DNA samples were subjected to standard two-dimensional gel electrophoreses. After development of an autoradiogram on a semi-dried gel, the gel area corresponding to the spot on the autoradiogram was punched out, and the DNA was recovered and cloned into a *NotI*-*HinfI* vector (18). After selection of bacterial clones, base sequences of the inserts were determined using ABI Prism 310 Genetic Analyzer (Applied Biosystems, Tokyo, Japan). Several clones were examined for each mutation and the consensus sequence reads were mapped on the mouse reference sequence, NCBI 37/mm9, using a basic local alignment search tool (BLAST)-like alignment tool or BLAT at Ensemble (http://www.ensembl.org/Mus_musculus/blastview). Chromosomal locations and upstream and downstream sequence information were obtained for each mutation.

Copy number estimation. SYBR® Green-based qPCR analyses were carried out using a LightCycler PCR system (Roche, Tokyo, Japan). The qPCR assays were performed according to the manufacturer's instructions. The assays were conducted in triplicates for each DNA sample of trio individuals (mutant offspring and the parents). The sequences of each primer are shown in Supplementary Table 1 (<http://dx.doi.org/RR3095.1.S1>).

Deletion size estimation. The size of each deletion was estimated by comparative genomic hybridization (CGH) analyses using Roche NimbleGen microarray systems. Whole-genome tiling arrays with 720 k probes were used with a mean distance between probes of about 1.4 kb. CGH experiments were carried out according to the manufacturer's instructions. The hybridized slides were scanned with a MS200 microarray scanner and the log₂ fluorescent ratio of each probe set was calculated with the NimbleScan and graphically plotted using SignalMap software.

Statistical Analysis

All observed numbers of mutations were treated as realizations of Poisson random variables characterized by a mutational rate expressed in terms of mutations per genome per generation, given here as percentage for convenience due to the small numbers involved. Confidence intervals for Table 3 were estimated by the "cii" procedure of Stata 11 statistical software (Stata Corporation, 2011). *P* values for the comparison of control and irradiated mice and comparisons of the BALB/c and B6C3 strains were calculated using the method based on assuming that the number of mutations in the irradiated group is distributed binomially and is conditional on the observed total number of mutations in both groups (19), with a "mid-*P*" correction for the discreteness of the observed values (20).

RESULTS

Selection of Spots for Mutation Analysis

In the present study, male B6C3 mice and female JF1 mice were used. Since the JF1 strain is somewhat distant evolutionally from laboratory mice, nearly half of the offsprings' spots consisted of single-copy spots that were unique to one parent. Consequently, the total number of

spots appearing in the autoradiograms of the offspring increased by nearly one-half (a total of about 2,000 spots) when compared with results from each parental strain.

To select appropriate spots for screening, a clear autoradiogram was chosen from both the 1–5 kb and 5–10 kb images (fragment lengths indicated in the first dimension gel run). These autoradiograms served as the master images for comparison with the spots observed in the autoradiogram images of the test samples: 958 (1–5 kb image) and 1,204 spots (5–10 kb image) were initially considered suitable for the screening because they did not overlap with the nearby spots, they were not located at a margin of the gel (where the appearance of such spot is not stable), and they did not consist of multiple copies (i.e., they were not large spots).

After examination of spot images of 50 test samples, those spots that were identified as polymorphic (i.e., either absent in some offspring or had a variation of approximately 50% in density among the offspring) were excluded. Finally, 864 spots (256 were unique single-copy spots derived from JF1 strain, 254 were unique single-copy spots from B6C3 strain and 354 were two-copy spots that were common to both strains) were selected for 1–5 kb images and 973 spots (391 were unique and derived from JF1, 343 were from B6C3, and 239 were common to both strains) were selected for the 5–10 kb images.

Crude Mutation Data

Two autoradiograms (1–5 kb and 5–10 kb images) from one F₁ mouse provided information on 1,190 (254 + 354 + 343 + 239) paternal fragments and 1,240 (256 + 354 + 391 + 239) maternal fragments (Fig. 1). The selected spots were examined in DNA samples from a total of 1,007 F₁ mice (505 from irradiated and 502 from unirradiated spermatogonia). A total of 595,387 irradiated paternal spots (505 F₁), 583,051 unirradiated paternal spots (502 F₁), and 1,288,352 unirradiated maternal spots (1,007 F₁) were finally subjected to mutation screening. The actual numbers were slightly smaller (by 1–2%) than expected since some parts of the gels were not suited for quantification of spot intensity.

A two-copy spot with normalized intensity below the chosen cut-off point (65% of mean value), or a single-copy spot that disappeared in an image from an offspring (where the parents displayed a spot within the normal intensity range) were considered as a mutation candidate. Subsequently, to exclude the possibility of mosaic mutations, which is unlikely to be derived from mutations from irradiated spermatogonia, kidney and liver DNA samples were used to confirm the observations made on spleen DNA samples. Two mutation candidates observed in experiments with spleen DNA samples were found as normal when DNA samples from kidney and liver of the same individuals were used. Therefore, these two were regarded as non-mutants and were excluded from further examinations. Also, the remaining candidate mutations were all confirmed

TABLE 1
Characteristics of the Mutations Detected

Mutation origin	Dose	Mouse ID	Mutation type	Spot ID affected	GenBank ID	Spot size (bp)	Spot location		
							Chromosome	Strand	Start (<i>NotI</i>)
Paternal	0 Gy	B6C3-0G-1	2.3-Mb deletion	S378	AB491227	749	10	+	122,422,557
				S893	AB491228	515	10	+	122,633,767
	4 Gy	B6C3-4G-1	10.6-Mb deletion	S280	AB491229	910	9	+	37,297,185
				S984	AB491230	443	6	+	90,938,614
		B6C3-4G-2	4.7-Mb deletion	S1592	AB491231	287	6	–	90,412,667
				L261	AB491232	968	6	+	92,656,006
				L1483	AB491233	338	6	+	90,412,741
				L400*	AB491234	845	13	+	101,386,885
		B6C3-4G-3	1.9-Mb deletion	L440*	AB491235	715	13	–	101,386,892
				S390	AB491236	860	6	–	99,642,935
		B6C3-4G-4	13-Mb deletion	S884	AB491237	519	6	+	99,643,396
				S1290*	AB491238	345	7	+	56,044,432
		B6C3-4G-5	4.3-Mb deletion	S1315*	AB491239	366	7	–	56,044,439
				S909	AB491240	513	7	+	50,484,981
	0 Gy	JF-0G-1	(CT) ₂₉ to (CT) ₃₂ (GT) ₃₂ to (GT) ₁₄	L700	AB491242	634	2	+	116,801,581

* L400 and L440, and S1290 and S1315 were derived from consecutive 3' and 5' fragments which contain common *NotI* sites.

in kidney and liver DNA samples. Finally, a total of 15 spots were found to be mutated in 8 animals: specifically, 12 spots were found in 6 mice from the exposed group and 3 spots were found in 2 mice from the control group (Table 1). The locations of these spots are indicated with arrows in Fig. 1, and patterns of normal and mutant spots are displayed in Fig. 2.

Characterization of Mutations

Parental origins of mutations. Identification of parental origins of deletions that occurred at single-copy spots (i.e., strain-specific spots) did not require any further molecular analyses. In contrast, two deletions observed in mice B6C3-4G-4 and B6C3-4G-5 involved two-copy spots common to both parental strains (Table 1) and hence determination of their parental origins required single nucleotide polymorphism (SNP) information in the deleted (or nondeleted) regions of the genome. For this purpose, a set of PCR primers were prepared at the 5' and 3' regions of the deletion breakpoints so that only the deleted alleles would

be amplified (the primer distances were designed to be at least several Mb apart so that PCR amplification would not work on normal DNA). The amplified products were sequenced and the deletion breakpoints were specified. Following a search of the Mouse Phenome Database at the Jackson Laboratory (<http://phenome.jax.org/>), SNP information was obtained in the deleted regions; four SNPs in the deletion of B6C3-4G-4 mouse and two in the deletion of B6C3-4G-5 mouse. Those SNP sites were PCR amplified, sequenced and compared with the SNP database to show that both deletions occurred in the irradiated paternal genome (Suppl. Table 2).

Microsatellite mutations. In two mutations, both occurred at single-copy spots, loss of the spot at a normal position was accompanied by the appearance of a novel single-copy spot near the original position (Fig. 2D). The appearance of such a new single-copy spot slightly above or below the original position is a hallmark of mutations at microsatellite sequences. In fact, sequencing of the DNA isolated from the normal and mutant spots revealed that one mutation resulted from a gain and the other from a loss of 2-base repeat units

TABLE 2
Sequences and the Locations of Breakpoints of Deletions Identified in the Exposed Group

Mouse ID (chromosome)	First breakpoint	Second breakpoint	Junction
B6C3-4G-1 (9)	TTCATGACTGcttc 31,956,359	cagt AGAGACACCC 42,515,497	TTCATGACTGAAGAGACACCC
B6C3-4G-2 (6)	GCACTCAGAGctat 89,709,524	cttGGAAAGATATT 94,405,362	GCACTCAGAGAAAGATATT
B6C3-4G-3 (13)	CTGTACCATGtcta 100,816,543	cagaAAGGGGATGC 102,748,640	CTGTACCATGAAGGGGATGC
B6C3-4G-4 (6)	TCTCTGAACtcggg 99,507,761	gggTTATTGGATTT 112,539,830	TCTCTGAACTTATTGGATTT
B6C3-4G-5 (7)	CAGACAACATttca 54,370,412	ggggGGAAATGTAA 58,625,965	CAGACAACATGGAAATGTAA

Note. Uppercase letters indicate retained nucleotides, lowercase letters indicate deleted nucleotides. Underlined bases were homologous between the first and second breakpoints. Breakpoint positions were the last 3' and first 5' retained nucleotides.

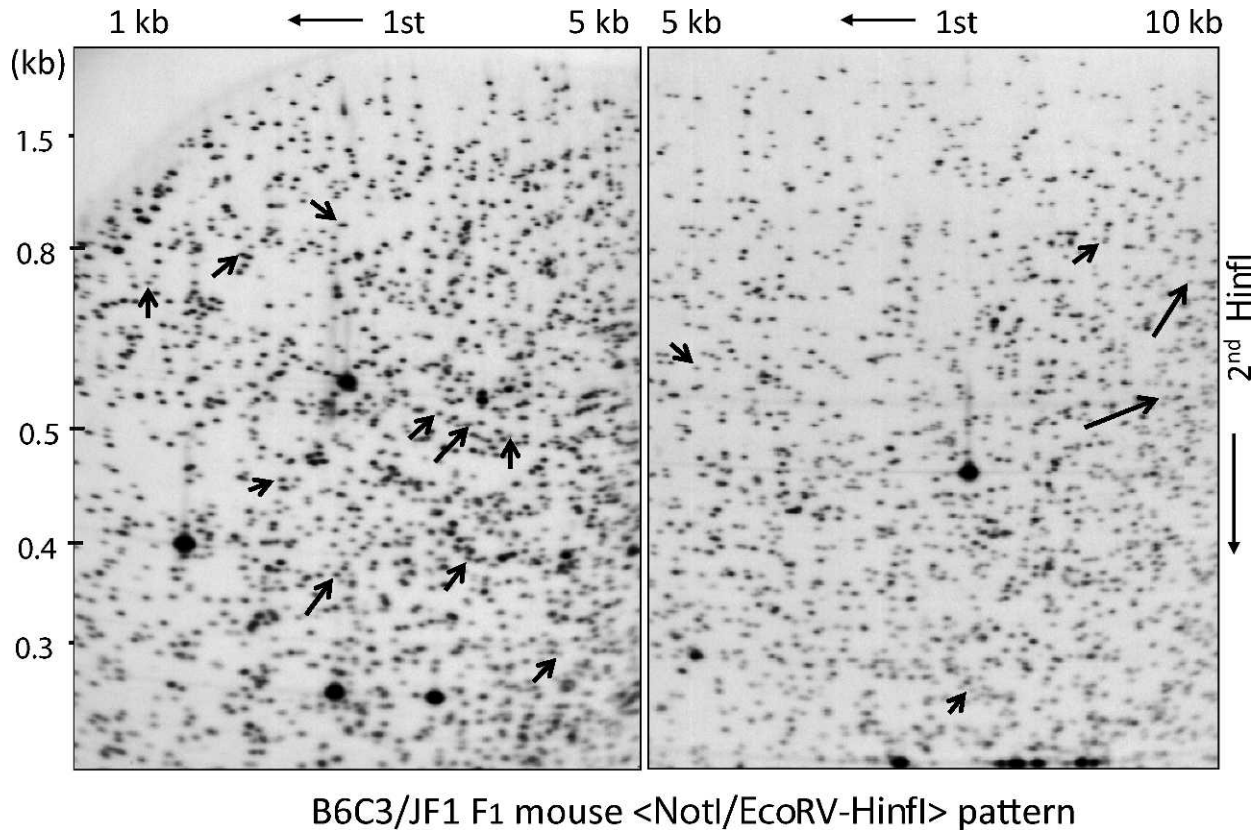


FIG. 1. RLGS patterns of mouse DNA. Spots that had undergone mutations are marked with arrows.

in microsatellite sequences (JF-0G-1 and B6C3-4G-6 mice, Table 1).

Deletion mutations. The remaining 13 spots showed decreased spot intensities but without any new spots. They were found among 6 mice, specifically, single spot was lost in 1 mouse, 2 spots each were lost in 4 mice, and 4 spots were lost in one mouse (Table 1). Since it seemed likely that the multiple losses of spots in each mouse was associated with a single event (i.e., a large deletion), sequencing data of the wild-type allele (with nonmutated spots) were used to determine their physical locations in the genome after an Ensemble BLAT search. The results showed that the reasoning was indeed correct. The two spots that were lost in B6C3-4G-3 and B6C3-4G-5 mice were 5' and 3' fragments originating from the same single *NotI* sites. Another mutant mouse (B6C3-4Gy-4) had lost 2 spots, while their *NotI* sites were only 462 bp apart on the same chromosome 6. Therefore, the 2 spots in these mutations were most likely included in one deletion. The remaining 2 mice (B6C3-0Gy-1 and B6C3-4Gy-2) had lost 2 and 4 spots, and the *NotI* sites were found to locate on the same chromosomes 10 and 6, respectively. Thus, these losses were also thought to be included in one large deletion, respectively, although the locations of the *NotI* sites were 210 kb and 2,245 kb apart from each other.

The copy numbers of such regions thought to be involved in large deletions were estimated by the qPCR assays. As shown in Fig. 3, the 6 candidate mutations were all found to carry only single copies (primers were set to amplify DNA fragments within the deleted spot), whereas all of the paternal samples had two copies. In one mutation that occurred in the B6C3-4G-5 mouse, DNA was not available from the mother, which, however, does not change the conclusion because the mutation is determined as being derived from the paternal genome by the SNP data.

To confirm that the simultaneous losses of multiple spots which were mapped on a single chromosome were caused by single deletions, the high-density array CGH technique was applied to three DNA samples harboring losses of multiple spots (B6C3-0Gy-1, B6C3-4Gy-2 and B6C3-4Gy-4 individuals). The results clearly demonstrated that each mutation was caused by a single large deletion (Fig. 4). Application of array CGH analysis to the remaining DNA samples allowed a rapid acquisition of approximate deletion size, which facilitated the subsequent determination of deletion breakpoints. The estimated deletion sizes are summarized in Table 1. It is clear that, regardless of the number of spots lost, deletions were on the order of megabases except for the mutations at microsatellite sequences.

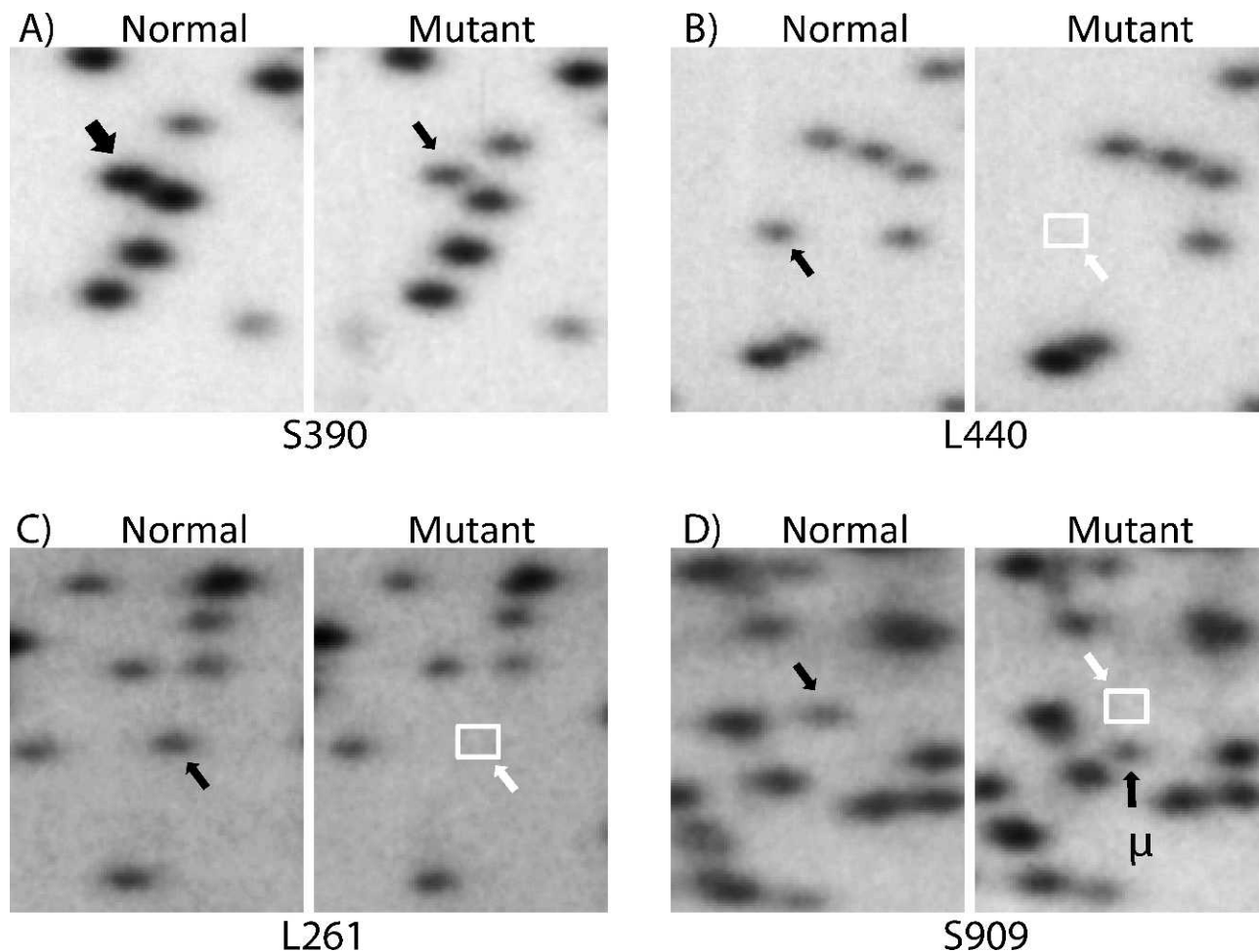


FIG. 2. Close-ups of RLGS patterns from normal and mutant DNA. Panel A: An example of the loss of one copy of DNA at a two copy spot (spot intensity was reduced by half). Panels B and C: Examples of the loss of a spot (indicated by white squares) that occurred at single copy spots. Panel D: An example of loss of a spot that accompanied a new spot (indicated by “ μ ”) near the normal position (indicated by a white arrow), an indication of a mutation at a repeat sequence. The numbers indicated below each panel represent the spot IDs in Table 1.

Characterization of breakpoint sequences. Since the six deletions found in the present study were all under heterozygous conditions, PCR primers were designed so that normal alleles were too long to be amplified, but only the mutated shorter alleles could undergo the amplification. The base sequences of the 5' upstream and 3' downstream of each deletion were also determined. We aligned their sequences on the reference mouse genome by BLAT search (UCSC Genome Browser: <http://genome.ucsc.edu/>) or ENSEMBL (Genome Browser: <http://www.ensembl.org/index.html>). One mutation found in the control group (B6C3-0G-1 mouse carrying a 2.3 Mb deletion) had truncated LINE-1 sequences of approximately 2 kb at both breakpoints. The results imply that the deletion occurred as a result of nonallelic homologous recombination (NAHR). The sequence information at the breakpoints of the remaining five deletions in the exposed group is given in Table 2. Two deletions had one-base homology between the two breakpoints, whereas the remaining three had no such

partial homology, indicating that they arose through nonhomologous end joining (NHEJ).

Other Findings

In addition to the 9 mice bearing germline deletion mutations, two mice had lost a number of single-copy spots.

Case 1. In one female mouse in the control group, 9 single-copy spots (all from the JF1 genome) were lost. Sequence data of these spots revealed that they all mapped to the X chromosome. Array CGH analysis indicated that this animal had only one X chromosome and no Y chromosome was present (i.e., monosomy X). It was confirmed that the X chromosome present in the offspring was derived from the B6C3 paternal mouse and hence it was the entire maternal X chromosome that was lost either before or after fertilization.

Case 2. Another female mouse also in the control group had lost 38 single-copy spots (all maternal). At the same time, 40 single-copy spots (all paternal) showed increased

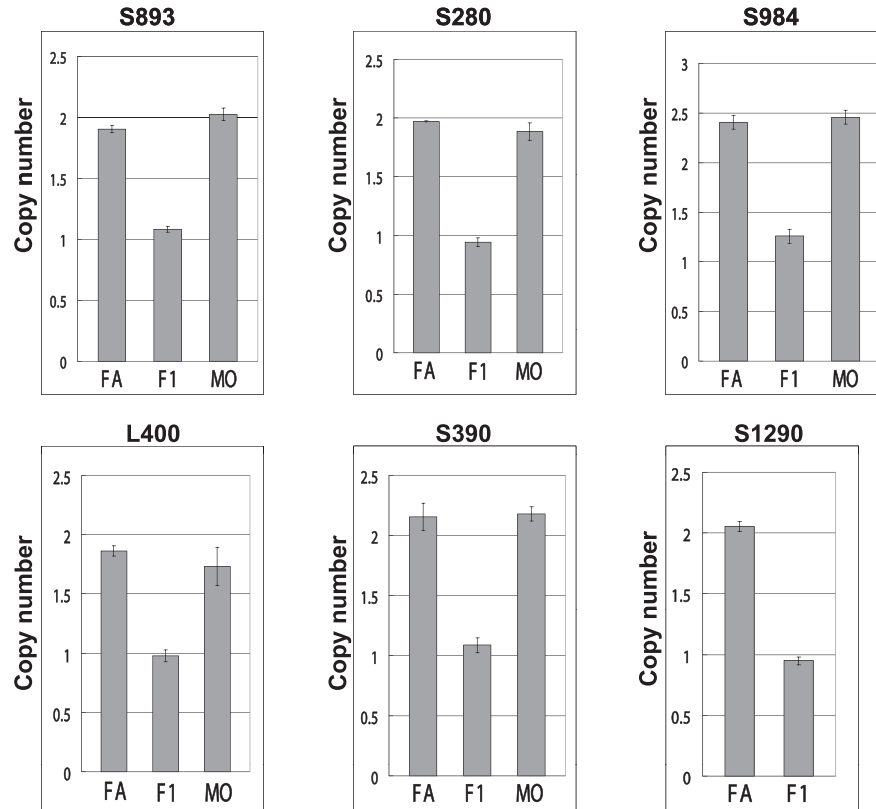


FIG. 3. Copy number estimates of the 6 deletion candidates. Paired PCR primers were set around the affected *NotI* sites. The spot numbers indicated on top of each panel represent the spot IDs shown in Table 1. The means of triplicate measures are shown. FA, F1 and MO stand for father, offspring and mother, respectively.

intensities similar to the level of two-copy spots. Cloning and sequencing analyses of DNA samples from 15 randomly selected spots among the 40 showed that they all mapped to the same chromosome 10. Array CGH analysis showed that chromosome 10 looked normal (i.e., two-copy signals) through the entire chromosome. These results indicated that the genome of this mouse consisted of two copies of paternal chromosome 10 and that no maternal chromosome 10 was present: specifically, this was a uniparental disomy (UPD). Since these two mutations are chromosomal events, they are not included in the estimate of mutation induction rate described below.

Radiation Effect

The present study found one paternally derived deletion mutation among 502 F₁ mice in the control group, which suggested a spontaneous mutation rate of 0.2% (95% CI, [0.028%, 1.4%]) under the present experimental conditions (screening of 1,190 paternally-derived spots per offspring). As five deletion mutations were found in the 505 offspring derived from the irradiated spermatogonia with 4 Gy, an induced mutation rate was estimated as 0.2% per Gy, with an approximate one-sided 95% CI, based on the assumption that the induced mutation rate cannot be <0, of [0, 0.40% per Gy]. Because the numbers of observed mutations were

small, the usual statistical theory for estimating a *P* value based on normal theory approximation may not be accurate in this case. Therefore, a number of methods were tried for estimating the *P* value for a difference between control and irradiated mice in the current study, as described more fully in “Statistical Analysis” in the Materials and Methods. Resulting estimates for the *P* value of a one-sided test were marginally significant, ranging from about 0.045–0.11, depending on the method used.

DISCUSSION

How to Define the Mutation Rate

In a previous study, the induced mutation rate was estimated by considering each *NotI* site to be equivalent to a gene in the specific-locus tests (i.e., the test used the ratio of the number of the affected *NotI* sites over the total number of *NotI* sites examined). However, several deletions were found to involve two adjacent fragments that shared the same *NotI* sites. Therefore, different estimations were made based on either the number of mutation events, the number of offspring, or the number of affected alleles (8). In the present study, two deletions involved single spots, whereas four deletions involved 2 spots and one deletion involved 4 spots (Table 1). Under

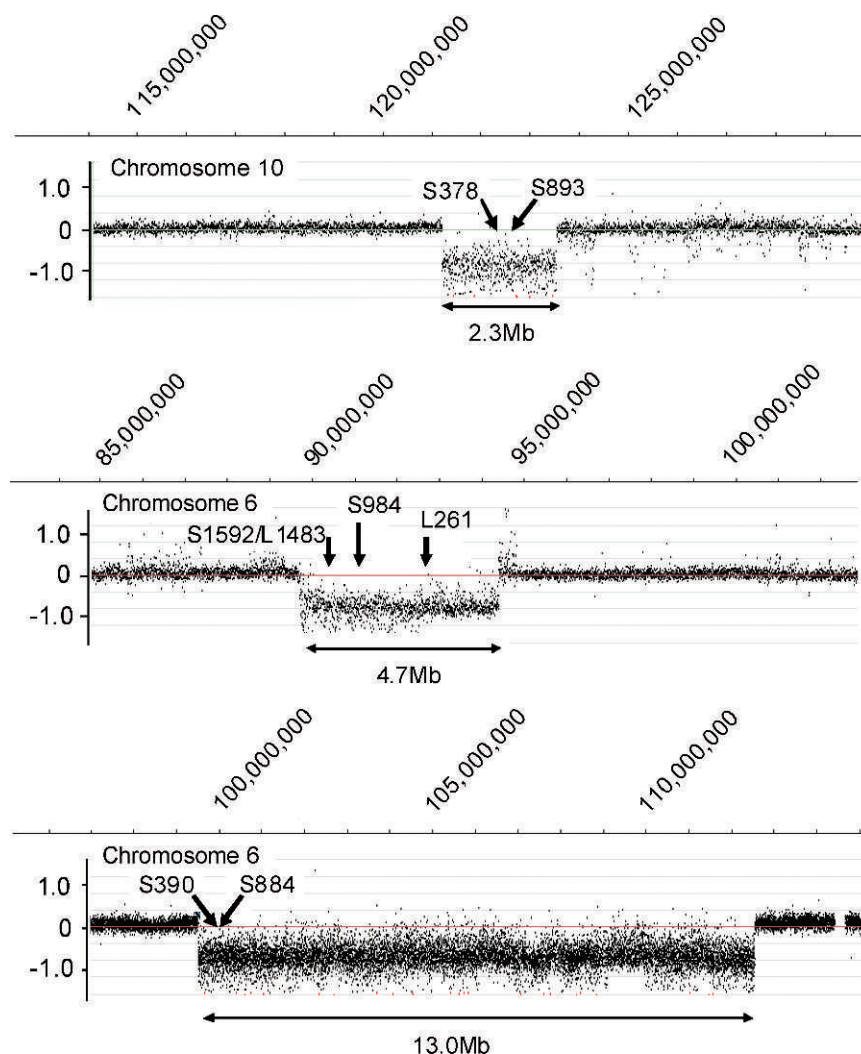


FIG. 4. Array CGH patterns of three mutations. The top panel represents the results of a B6C3-0G-1 mouse, the middle panel represents a B6C3-4G-2 mouse and the lower panel represents a B6C3-4G-4 mouse. Arrows indicate locations of *NotI* sites in the deletions.

such conditions, it does not seem appropriate to define the mutation induction rate in terms of the *NotI* site, because the loss of a single *NotI* site n times independently is not the equivalent of the loss of n *NotI* sites within one deletion (i.e., a single event). Consequently, the present study should be considered as a specific-locus test involving 14 *NotI* sites that have undergone deletion mutations, and the mutation induction rate should be estimated as the number of deletion events per genome. In the following discussions, mutations at microsatellite sequences will be excluded from the radiation-induced mutations. Likewise, insertions or deletions of transposon sequences and uniparental disomy will also be excluded.

Possible Radiation Sensitivity of the BALB/c Strain

Since we used two strains for irradiation, BALB/c and B6C3, and the BALB/c strain is known to carry a mutation at the DNA-PK gene (13), it was interesting to compare the two

sets of data (Table 3). Although the results for the BALB/c strain may look consistently higher than the results for the B6C3 strain, the data sets are not large enough to indicate a statistical significance either in the unexposed or the exposed groups. It should be mentioned that RLGS studies with mice numbering about 1,000 are not sufficient to indicate that BALB/c mice are more sensitive to radiation for mutation induction in spermatogonia. These results are in line with the results of studies at repair kinetics for radiation-induced DNA double-strand breaks (observed as γ H2AX foci): namely, the kinetics were only slightly slower in BALB/c-derived cells compared with B6C3-derived cells (21).

Estimation of the Mutation Induction Rate

Present results showed one deletion mutation in the control group ($n = 502$) and five deletion mutations in the exposed group ($n = 505$, 4 Gy dose) (Table 1). Thus, the crude rate of detecting a deletion mutation is about 0.2% per Gy (i.e., one

TABLE 3
Summary of Previous Results (Experiment 1) (8) and Present Results (Experiment 2)

Experiment	Irradiated strain	Dose	No. F ₁ mice	Number of deletions relevant to the risk of paternal genome	Estimated mutation frequency in spermatogonia [CI]
1	BALB/c	0 Gy	190	1*	1/190 = 0.53% [0.013%, 2.9%]
1	BALB/c	3 Gy	237	3	3/237 = 1.3% [0.26%, 3.7%]
1	BALB/c	5 Gy	79	1	1/79 = 1.3% [0.032%, 7.1%]
2	B6C3	0 Gy	502	1	1/502 = 0.20% [0.005%, 1.1%]
2	B6C3	4 Gy	505	5	5/505 = 0.99% [0.32%, 2.3%]

* There were 2 identical deletions (clonal events), but the parental origins could not be determined. Therefore, the parental origins of the two deletions were assumed to be derived equally from the paternal and maternal genomes.

animal among 500 examined). Since the estimated number of coding genes is about 25,000 per genome (22), or about 25× the number of the 1,190 *NotI* sites examined here, the probability of a deletion mutation (detectable with the RLGS method) that includes any coding gene of the genome is estimated by multiplying the induction rate (0.2%) by 25 or 0.05 (5%) per haploid genome. Another approach is based on the estimation that the present RLGS technique screens about 0.2% of the genome (i.e., the mean fragment size in the first dimension gel is 5 kb and 1,190 spots × 5 kb = 6,000 kb, which is 0.2% of the haploid genome of 3,000 Mb). Therefore, multiplying the mutation induction rate of 0.2% by 500 (i.e., 1/0.002) gives a probability of 100% or 1, for the probability of a deletion mutation occurring any place in the genome following exposure of spermatogonia cells to 1 Gy.

In contrast, Russell's 7 locus tests gave an estimated mutation rate of $\sim 2 \times 10^{-5}$ /locus per Gy, while UNSCEAR estimated a mean of 1.08×10^{-5} /locus per Gy following the inclusion of 29 additional genes (for a total of 36 genes) (7). When the number of coding genes (i.e., 25,000) is multiplied by the mean mutation induction rate per locus, an estimate of 0.25 (25%) is obtained (i.e., 1×10^{-5} /locus × 25,000 genes/genome), which represents the probability that a coding gene is involved in a mutation (not necessarily a large deletion) after exposure of spermatogonia cells to 1 Gy.

The estimated probability of any gene of a genome undergoing mutation appears roughly 5× larger when based on the specific-locus data (25%) compared with that on the RLGS data (5%). The difference may be simply due to statistical fluctuation in the small number of mutants observed in the present study, but can also be explained by the higher sensitivity of the mutation detection in the specific-locus test. Namely, this is a functional test of specific genes, and therefore any kind of mutation that inactivates the normal function can be detected, including base substitutions, deletions of a few bases and also inversions, which are mostly not detectable with the RLGS method. In contrast, the detection of deletions/insertions with the RLGS method usually requires size alterations of 5% or larger of the DNA fragments during the second dimension electrophoresis (fragments range between 300–2,000 bp): namely, ~ 15 bp or larger.

The difference between the two estimates may become even smaller if the analyses were restricted to possible large deletions detected in the specific locus tests. Specifically, it is reported that about one-third ($29/76 = 0.38$) of radiation-induced alleles are lethal under homozygous conditions, which is probably due to inclusion of adjacent essential gene(s) in the deletion (Table XV of Searles's review, see ref. 23). In this calculation, results for *d* and *s* loci were excluded because their nonfunctional (but intragenic) alleles were later found to be homozygous lethal (24, 25). As a consequence, the above mentioned 5× difference in the estimated mutation induction rate between the specific-locus test and the RLGS method may be reduced to about 2× difference when possible deletions are compared. It is impressive that the two totally different systems for detection of germline mutations in mice provide estimated risks of mutations (or deletions) in a coding gene that are within 2–5× difference (5% by RLGS, 25% by specific locus tests and 7% when specific locus data were restricted to homozygous lethal mutations). The major finding following a genome-wide search of mutations with the RLGS method is that deletion mutations are not easily induced in the genome. This is potentially good news for humans, concerned about radiation-induced germline mutations, but will require researchers to move ahead with further sophisticated systems such as micro array-based CGH, and ultimately whole genome sequencing to truly estimate the mutation induction rate in mammalian germ cells.

Future Directions

The Human Genome Project was completed in 2003, and research interests have shifted toward analysis of individual differences in the human genome. Studies to date indicated that the human genome has already accumulated a large number of mutations, e.g., more than one million SNPs, several hundred thousand deletions/insertions (copy number variations, CNV) and several hundred deletion/insertion events in coding exons. The genome of James Watson contains dozens of genes that are likely to be nonfunctioning (26) however these apparently nonfunctioning genes could possibly function under heterozygous conditions because the normal alleles could have failed to be sequenced by chance due to lower coverage of the sequences of their positions. Our

results using RLGS indicate that the number of new mutational events (deletions) induced by an acute exposure of 1 Gy (which is rare, even assuming accidental exposure conditions) is probably 1 or fewer per genome. Since the human genome already contains many CNVs, adding one additional deletion to the genome *per se* may not be seem critically detrimental. Rather, the nature of specific genes involved in a deletion may be more important than the fact of a deletion. In this context, it is important to know the proportion of genes with and without health effects under hemizygous conditions (i.e., deletion heterozygotes). The former are represented as mutations at haplo-insufficient genes and the latter as haplo-sufficient genes. In addition, recent genome sequencing studies indicated that an ordinary individual carries 250–300 nonfunctioning alleles and 50–100 variations that are possibly disease related (27). Some studies even indicated that each genome contained 30 to over 100 genes that appeared as mutation homozygotes (loss-of-function state) (e.g., 28, 29). Through such genome sequencing studies of clinically normal individuals, it is expected that a list of haplo-sufficient genes would increase rapidly in the near future, while a list of potentially haplo-insufficient genes would require more effort and time. The proportion of the latter will be helpful for further evaluation of genetic risks of radiation.

In conclusion, the time has come to recognize the fact that the human genome has already accumulated a large number of mutations of different kinds. Therefore, risk evaluation needs to incorporate this important information (as a baseline) so that additional genetic risks from radiation may be put into perspective, and thereby better understood by the public.

ACKNOWLEDGMENT

We thank Y. Nakamoto, S. Kaneoka, T. Tsuji, A. Miura, S. Mishima, K. Naito, J. Kaneko, M. Imanaka and H. Haba for their technical assistance, and Dr. L. Kapp for his careful reading of the manuscript. We thank Dr. T. Shiroishi at the National Institute of Genetics for providing the JF1 mice. The Radiation Effects Research Foundation (RERF), Hiroshima and Nagasaki, Japan is a private, nonprofit foundation funded by the Japanese Ministry of Health, Labour and Welfare and U.S. Department of Energy (DOE), the latter in part through DOE Award DE-HS0000031 to the National Academy of Sciences. This publication was supported by RERF Research Protocols RP 7–85 and RP 2–07. A part of this work was supported by MEXT KAKENHI 20312033 to JA. The views of the authors do not necessarily reflect those of the two governments.

Received: June 7, 2012; accepted: October 9, 2012; published online: January 31, 2013

REFERENCES

1. Preston DL, Ron E, Tokuoka S, Funamoto S, Nishi N, Soda M, et al. Solid cancer incidence in atomic bomb survivors: 1958–1998. *Radiat Res* 2007; 168:1–64.
2. Ozasa K, Shimizu Y, Suyama A, Kasagi F, Soda M, Grant EJ, et al. Studies of the mortality of atomic bomb survivors, Report 14, 1950–2003: An overview on cancer and noncancer diseases. *Radiat Res* 2012; 177:229–43.
3. Shimizu Y, Kodama K, Nishi N, Kasagi F, Suyama A, Soda M, et al. Radiation exposure and circulatory disease risk: Hiroshima and Nagasaki atomic bomb survivor data, 1950–2003. *Br Med J* 2010; 340:b5349. doi: 10.1136/bmj.b5349.
4. Nakamura N. Genetic effects of radiation in atomic-bomb survivors and their children: Past, present and future. *J Radiat Res* 2006; 47(Suppl. B):B67–73.
5. Winther JF, Boice Jr. JD, Frederiksen K, Bautz A, Mulvihill JJ, Stovall M, et al. Radiotherapy for childhood cancer and risk for congenital malformations in offspring: a population-based cohort study. *Clin Genet* 2009; 75:50–6.
6. Green DM, Lange JM, Peabody EM, Grigorieva NN, Peterson SM, Kalapurakal JA, et al. Pregnancy outcome after treatment for Wilms tumor: a report from the national Wilms tumor long-term follow-up study. *J Clin Oncol* 2010; 28:2824–30.
7. United Nations Scientific Committee on the Effects of Atomic Radiation (UNSCEAR). Hereditary Effects of Radiation (2001 Report): United Nations; 2001.
8. Asakawa J, Kuick R, M. Kodaira M, Nakamura N, Katayama H, Pierce D, et al. A genome scanning approach to assess the genetic effects of radiation in mice and humans. *Radiat Res* 2004; 161:380–90.
9. Asakawa J, Kuick R, Neel JV, Kodaira M, Satoh C, Hanash SM. Genetic variation detected by quantitative analysis of end-labeled genomic DNA fragments. *Proc Natl Acad Sci U S A* 1994; 91:9052–6.
10. Bird A, Taggart M, Frommer M, Miller OJ, Macleod D. A fraction of the mouse genome that is derived from islands of non-methylated, CpG-rich DNA. *Cell* 1985; 40(1):91–9.
11. Larsen F, Gundersen G, Lopez R, Prydz H. 1992, CpG islands as gene markers in the human genome. *Genomics* 13(4):1095–107.
12. Asakawa J, Nakamura N, Katayama H, Cullings HM. Estimation of mutation induction rates in AT-rich sequences using a genome scanning approach after X irradiation of mouse spermatogonia. *Radiat Res* 2007; 168(2):158–67.
13. Okayasu R, Suetomi K, Yu Y, Silver A, Bedford JS, Cox R, et al. A deficiency in DNA repair and DNA-PKcs expression in the radiosensitive BALB/c mouse. *Cancer Res* 2000; 60:4342–5.
14. Koide T, Moriwaki K, Uchida K, Mita A, Sagai T, Yonekawa H, et al. A new inbred strain JF1 established from Japanese fancy mouse carrying the classic piebald allele. *Mamm Genome* 1998; 9:15–9.
15. Kuick R, Asakawa J, Neel JV, Satoh C, Hanash SM. High yield of restriction fragment length polymorphisms in two-dimensional separations of human genomic DNA. *Genomics* 1995; 25:345–53.
16. Asakawa J. Restriction landmark genome scanning for the detection of mutations. In: Cristofre Martin, editor. *Methods in molecular biology. Environmental genomics*. New Jersey: Humana Press; 2007. P. 153–70.
17. Kuick RD, Skolnick MM, Hanash SM, Neel JV. A two-dimensional electrophoresis-related laboratory information processing system: Spot matching. *Electrophoresis* 1991; 12:736–46.
18. Thoraval D, Asakawa J, Kodaira M, Chang C, Radany E, Kuick R, et al. A methylated human 9-kb repetitive sequence on acrocentric chromosomes is homologous to a subtelomeric repeat in chimpanzees. *Proc Natl Acad Sci U S A* 1996; 93:4442–7.
19. Shiu W, Bain L. Experiment size and power comparisons for two-sample Poisson tests. *Appl Stat* 1982; 31:130–4.
20. Lancaster HO. The combination of probabilities arising from data in discrete distributions. *Biometrika* 1949; 36:370–82.
21. Fabre KM, Ramaiah L, Dregalla RC, Desaintes C, Weil MM, Bailey SM, et al. Murine Prkdc polymorphisms impact DNA-PKcs function. *Radiat Res* 2011; 175: 493–500.
22. Waterston RH, et al. Mouse Genome Sequencing Consortium. Initial sequencing and comparative analysis of the mouse genome. *Nature* 2002; 420:520–62.

23. Searle AG, Mutation induction in mice. *Adv Radiat Biol* 1974; 4:131–207.
24. Hosoda K, Hammer RE, Richardson JA, Baynash AG, Cheung JC, Giaid A, et al. Targeted and natural (piebald-lethal) mutations of endothelin-B receptor gene produce megacolon associated with spotted coat color in mice. *Cell* 1994; 79:1267–76.
25. Strobel MC, Seperack PK, Copeland NG, Jenkins NA. Molecular analysis of two mouse dilute locus deletion mutations: spontaneous dilute lethal20J and radiation-induced dilute prenatal lethal Aa2 alleles. *Mol Cell Biol* 1990; 10:501–9.
26. Wheeler DA, Srinivasan M, Egholm M, Shen Y, Chen L, McGuire A, et al. The complete genome of an individual by massively parallel DNA sequencing. *Nature* 2008; 452:872–6.
27. The 1000 Genomes Project Consortium. A map of human genome variation from population-scale sequencing. *Nature* 2010; 467:1061–73.
28. Pelak K, Shianna KV, Ge D, Maia JM, Zhu M, Smith JP, et al. The characterization of twenty sequenced human genomes. *PLoS Genet* 2010; 6. pii: e1001111.
29. MacArthur DG, Tyler-Smith C. Loss-of-function variants in the genomes of healthy humans. *Hum Mol Genet* 2010; 19:R125–30.